Available online at www.sciencedirect.com
ScienceDirect
Polymer 48 (2007) 1998–2006
polymer
www.elsevier.com/locate/polymer

Influence of morphology on the properties of segmented block copolymers

Martijn J. van der Schuur[1], Reinoud J. Gaymans*

Department of Science and Technology, Twente University, P.O. Box 217, 7500 AE Enschede, The Netherlands

Received 17 October 2006; received in revised form 16 January 2007; accepted 30 January 2007
Available online 1 February 2007

Abstract

A comparison was carried out regarding the structure and properties of segmented block copolymers with either non-crystallisable or crystallisable rigid segments. The flexible segment in the block copolymers was a linear poly(propylene oxide) end capped with poly(ethylene oxide), with a segment molecular weight of 2300 g/mol. The rigid segments were either non-crystallisable or monodisperse crystallisable polyamides of varying lengths. The morphologies were studied by TEM and AFM, the thermal mechanical properties by DMA and the elastic properties by compression set and tensile measurements. A direct comparison was made of segmented block copolymers with either liquid–liquid demixed or crystallised structures. The crystallised amide segments were more efficient in increasing the modulus and improving the elastic properties than the non-crystallisable ones. The copolymers with crystallised structures were transparent, had a low glass transition temperature of the polyether phase and a modulus that was independent of temperature between T_g and T_m. These copolymers also displayed a very low loss factor (tan δ), suggesting excellent dynamic properties. The hard phase in segmented block copolymers should thus preferably be crystalline.

Keywords: Segmented; Liquid–liquid demixed; Crystallised

1. Introduction

Segmented block copolymers are often combined of flexible and rigid segments, where the rigid segments have a tendency to phase separate. At room temperature, these segmented block copolymers have multi-phase structures consisting of a continuous low-T_g phase of the flexible segments and a dispersed phase with a high melting temperature. The temperature range for their utilization is situated between the low glass transition temperature and the high melting temperature (flow temperature). Moreover, these linear copolymers are easily melt processable above their flow temperature (T_{flow}). The phase separation of the hard phase can occur either by liquid–liquid demixing, through the formation of hard spheres, and/or by crystallisation of crystalline lamellae or ribbons with high aspect ratios [1–5]. Liquid–liquid demixing takes place in a binary polymer system when the product of the Flory–Huggins interaction parameter, χ, and the degree of polymerization, N, exceed a critical value [6]. Thus, on increasing the length of either the flexible or the rigid segments, phase separation can be induced. Liquid–liquid demixing is a slow process as compared to crystallisation [7] and occurs in the melt during the polymerization. This is also known as melt phasing [8–10]. Crystallisation of the rigid segments is possible if their structure is regular, as for certain polyurethane, polyester and polyamide segments. The part of the rigid segments that is not demixed or crystallised remains dissolved in the soft phase and consequently causes an increase in the glass transition temperature of that phase.

The phase-separated rigid segments have two functions: they act as physical crosslinks (network points) and as filler particles (reinforcement) [11–13]. The reinforcing effect of spherical filler particles on the (storage) modulus of a material can be described by the Guth–Smallwood relation [14]. The

* Corresponding author.
E-mail addresses: mvds@oce.nl (M.J. van der Schuur), r.j.gaymans@utwente.nl (R.J. Gaymans).
[1] Present address: Océ-Technologies B.V., 5900 MA Venlo, The Netherlands.

0032-3861/$ - see front matter © 2007 Elsevier Ltd. All rights reserved.
doi:10.1016/j.polymer.2007.01.063

reinforcing effect of the crystallites, on the other hand, can be described by a polymer–fibre composite model with a random fibre orientation such as proposed by Halpin–Tsai [15,16]. The reinforcing effect of the fibres is dependant on the moduli of the phases, as well as the concentration and the aspect ratio of the crystallites.

In polyester-segmented block copolymers the phase separation occurs mainly by crystallisation, whereas a combination of liquid–liquid demixing and crystallisation occurs for polyurethane- and polyamide-segmented copolymers [1]. A direct comparison of the properties of a system that is merely liquid–liquid demixed or merely crystallised has, to the best of our knowledge, not been performed. In order to obtain liquid–liquid demixing without crystallisation, one can use hard segments with an irregular structure, so as not to crystallise, but with lengths long enough to demix. Crystallisation without liquid–liquid demixing can be obtained with hard segments with very regular structures leading to an easy crystallisation, but with segment lengths short enough in order not to demix. Thus, by using short monodisperse crystallisable segments, liquid–liquid demixing can be avoided, at the same time as a large fraction of the segments crystallise [12,13,17,18].

In the present study, the effect of morphology on the material properties was investigated by keeping the concentration of the flexible segments constant while increasing that of the rigid segments. A linear poly(propylene oxide) end capped with poly(ethylene oxide) with a molecular weight of 2300 g/mol was chosen as the flexible segment, and the rigid ones were made up of amide segments resembling polyurethanes (Fig. 1).

Amide bonds are far more thermally stable as compared to urethane and urea bonds, which is what made this study possible. The amide segments were coupled to the polyether segments by ester groups. The non-crystallising segment was based on poly(*m*-xylylene isophthalamide) with a random length distribution (*m*-PEEA). The segment length (x) of the poly(*m*-xylylene isophthalamide) was 2.5–10. At a segment length of 2, the difference in structure and properties of a random vs. a uniform length of poly(*m*-xylylene isophthalamide) was small [11]. From this, it was expected that the segment length distribution was not critical for the phase structure of non-crystallising systems. However, for liquid–liquid demixing to take place, the length x should be at least 2.5.

Short monodisperse segments of the regular poly(*p*-xylylene terephthalamide) (*p*-PEEA) and poly(hexamethylene terephthalamide) (6-PEEA) were selected as crystallising segments. These short monodisperse crystallisable segments had very high crystallisation rates as well as high crystallinities [12,13,17,18]. As all the segments were of the same length, the crystallites were expected to be uniform in thickness. The properties of these copolymers have been studied in previous investigations [11–13] and the present study presents a direct comparison of the systems with regard to their well-defined morphologies.

2. Experimental

2.1. Materials

The synthesis of the segmented block copolymers PEO–PPO–PEO–*m*-PEEA [11], PEO–PPO–PEO–*p*-PEEA [12] and PEO–PPO–PEO–6-PEEA [13] has been described elsewhere.

2.2. Viscometry

The inherent viscosities of the polymer samples were measured at a concentration of 0.1 g/dl in phenol/1,1,2,2-tetrachloroethane (1:1 molar mixture) at 25 °C using a capillary Ubbelohde 1B.

2.3. Transmission electron microscopy (TEM)

A small drop (40 μl) of a 0.3 wt% solution of polymer in hexafluoro isopropanol (HFIP) was cast on a carbon coated copper grid (200 mesh). Subsequently, the grid with the polymer film was heated at 20 °C/min to 20 °C above the flow temperature and maintained at the same temperature for 10 min. Subsequently, the material was allowed to cool at 3 °C/min

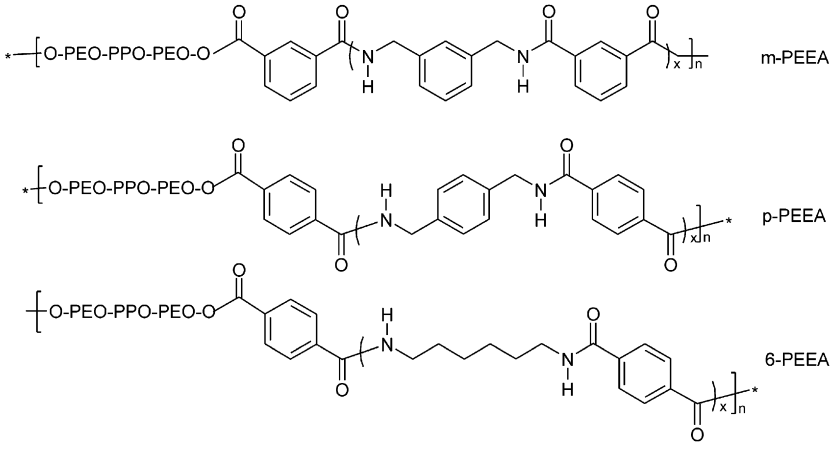

Fig. 1. Structures of *m*-PEEA, *p*-PEEA and 6-PEEA.

to 40 °C below the melting temperature. At this temperature, the samples were annealed for 10 min after which the sample was allowed to cool to room temperature at 3 °C/min. The treated samples were stained with 1 wt% osmium tetroxide/formaldehyde solution for 1 h at 40 °C. TEM measurements were performed on a Phillips CM30 at an accelerating voltage of 300 kV.

2.4. Atomic force microscopy

AFM measurements were performed on a Nanoscope IV controller (Veeco Instruments Inc., Woodbury, NY) operating in tapping mode. The AFM was equipped with a J-scanner with a maximum size of 200 μm^2 and Si cantilevers were used to obtain height and phase images. The amplitude in free oscillation was 5.0 V. The operating setpoint value (A/A_0) was set to a relative low value (0.7). Solvent-cast samples of ~150 μm were prepared from a 10 wt% solution in TFA. None of the samples were heat treated.

2.5. Injection moulding

Test specimens, i.e. bars of $70 \times 9 \times 2\ mm^3$ size, were prepared by injection moulding using an Arburg H manual injection moulding machine. The barrel temperature was set to approximately 50 °C above the flow temperature. The injection moulded test bars were stored at room temperature for about two weeks awaiting further experiments. All samples were dried overnight in vacuo at 70 °C before use.

2.6. Dynamic mechanical thermal analysis (DMA)

The storage (G') and loss (G'') moduli as functions of temperature were measured on the injection moulded test bars ($70 \times 9 \times 2\ mm^3$) with a Myrenne ATM3 torsion pendulum operating at a frequency of 1 Hz. The samples were first cooled to −100 °C and then heated at a rate of 1 °C/min with a 0.1% strain. The temperature at the maximum of the loss modulus was taken as the glass transition temperature. The flow or softening temperature (T_{flow}) was defined as the temperature where the storage modulus reached 1.0 MPa. The flex temperature (T_{flex}) was defined as the temperature at the start of the rubber plateau region.

2.7. Compression set

The samples for compression set were cut from the injection moulded bars. The compression set was measured according to the ASTM 395 B standard. The entirety of the experiment was carried out at room temperature. After 24 h with a compression of 25%, the pressure was released and half an hour later, the thickness of the samples was measured. The compression set was taken as the average of three measurements and was defined as

$$CS = \frac{d_0 - d_2}{d_0 - d_1} \times 100\% \quad (1)$$

where d_0 is the thickness before compression (mm); d_1 is compressed thickness (mm) (here $d_1 = 1.65$ mm); d_2 is thickness one hour after release of compression (mm).

2.8. Tensile set

Cyclic stress–strain experiments were carried out on the injection moulded bars cut to dumbbells (ISO 37 s3). A Zwick Z020 universal tensile machine equipped with a 500 N load cell was used to measure the stress as a function of strain at a strain rate of $3.33 \times 10^{-2}\ s^{-1}$ (corresponding to a test speed of 50 mm/min). The strain of each loading–unloading cycle was increased (staircase loading) and the incremental tensile set was determined as a function of the applied strain. No holding time was added between the cycles. The incremental tensile set was calculated from the following relation.

$$\text{Tensile set} = \frac{\Delta\varepsilon_{\text{remaining}}}{\Delta\varepsilon_{\text{cycle}}} = \frac{\varepsilon_{\text{r,cycle}(i)} - \varepsilon_{\text{r,cycle}(i-1)}}{\Delta\varepsilon_{\text{cycle}}} \times 100\% \quad (2)$$

Here, $\varepsilon_{\text{r,cycle}(i)}$ represents the remaining strain at the end of cycle i and $\varepsilon_{\text{r,cycle}(i-1)}$ is the remaining strain at the end of the preceding cycle $i-1$. A new cycle was started directly after the stress had decreased to zero and the strain steps were 20%.

3. Results and discussion

Segmented block copolymers based on polypropylene oxide and amide segments were synthesised. The amide segments were poly(*m*-xylylene isophthalamide) (*m*-PEEA) [11], poly(*p*-xylylene terephthalamide) (*p*-PEEA) [12] and poly(hexamethylene terephthalamide) (6-PEEA) [13] (Fig. 1). The poly(*m*-xylylene isophthalamide) had an irregular structure, a relatively large length ($x = 2.5–10$), a random length distribution and consequently these segments did not crystallise. At shorter lengths, the amide segments remained dissolved in the ether phase and the copolymer was a liquid at room temperature. The effect of polydispersity on the phase separation of poly(*m*-xylylene isophthalamide) segments was small [11].

Poly(*p*-xylylene terephthalamide) and poly(hexamethylene terephthalamide) had regular structures, short segment lengths ($x = 1–3$) and the segments also had monodisperse distributions. The coupling between the polyether and the amide segments took place through ester groups. The polypropylene oxide was end capped with polyethylene oxide (PEO–PPO–PEO_{2300}) and had a molecular weight of 2300 g/mol. As a result of the PEO end caps, all the hydroxylic end groups were primary alcohols. Primary alcohols are more reactive than secondary ones, enabling the formation of linear, high molecular weight polymers in an ester synthesis [19]. Table 1 summarises some properties of these copolymers. The inherent viscosities of the copolymers decreased with increasing length of the amide segment. Consequently, the miscibility of the PPO and amide segments also decreased and there was a chance melt phasing had taken place during the polymerization. A non-homogeneous polymerization often results in lower molecular weights.

Table 1
Some properties of the PEEA-segmented block copolymers

	x[a]	wt%[b]	vol%[c]	Structure[d]	Visc. (dl/g)	T_g (°C)	T_{flex} (°C)	T_{flow} (°C)	$G'_{25\,°C}$ (MPa)	$\Delta G'$ (−)	$CS_{25\%}$ (−)	$TS_{50\%}$ (−)
m-PEEA	2.5	24.6	19.7	Spheres	1.43	−53	−25	130	1.9	31	60	
	3	27.6	22.3	Spheres	1.62	−55	−20	120	3.7	30	50	37
	4	32.8	26.9	Spheres	0.43	−52	−30	127	5.5	23	50	
	5	37.4	31.0	Spheres	0.53	−50	−25	110	5.6	28	44	35
	6	41.3	34.6	Spheres	1.19	−51	−35	175	12	13	12	25
	8	48.0	41.0	Spheres	0.87	−52	−35	177	21	11	23	21
	10	53.0	46.0	Spheres	0.66	−51	−35	195	47	8.4	17	19
p-PEEA	1	12.1	8.6	Ribbons	1.89	−60	−44	60	18	1.4	37	18
	2	19.5	14.2	Ribbons	1.14	−65	−53	215	22	0	11	9
6-PEEA	1	12.0	8.5	Ribbons	1.92	−66	−51	85	11	6	29	31
	2	19.4	14.1	Ribbons	1.03	−61	−46	194	28	0	13	17
	3	25.7	19.0	Ribbons	0.67	−61	−40	264	30	0	11	13

[a] x is the amide repeat length.
[b] Amide wt%.
[c] Amide vol%.
[d] Amide phase morphology.

3.1. Morphology

3.1.1. m-PEEA

The irregular poly(*m*-xylylene isophthalamide) segments in *m*-PEEA (Fig. 1a) were found not to crystallise. These amide segments with more than two repeat units gave rise to cloudy melts during the polymerization at 250 °C. The resulting co-polymers were non-transparent solids at room temperature [11]. For amide segment lengths longer that two repeat units, phase separation took place by liquid−liquid demixing (Fig. 2a). The extended length of the amide segments ranged from 5.5 to 20.3 nm. In the TEM micrographs of these *m*-PEEA copolymers, submicron (30−500 nm) spherical domains were visible as were several nano-domains (3−10 nm). The nano-domains were believed to consist of coiled amide segments. As a result of the submicron domains being much larger than the amide segment length, they must also contain ether segments, resulting in a salami-type morphology. The non-phase-separated amide segments were dissolved in the polyether phase. Thus, dissolved amide segments, dispersed nanoparticles and dispersed salami-type submicron particles were present in the polyether matrix. The submicron salami-type particles consisted of a matrix of polyamide with dispersed polyether segments.

AFM analysis on the *m*-PEEA structure was inconclusive. This was probably a result of the difference in hardness of the phases being too small to be observed in the phase angle mode.

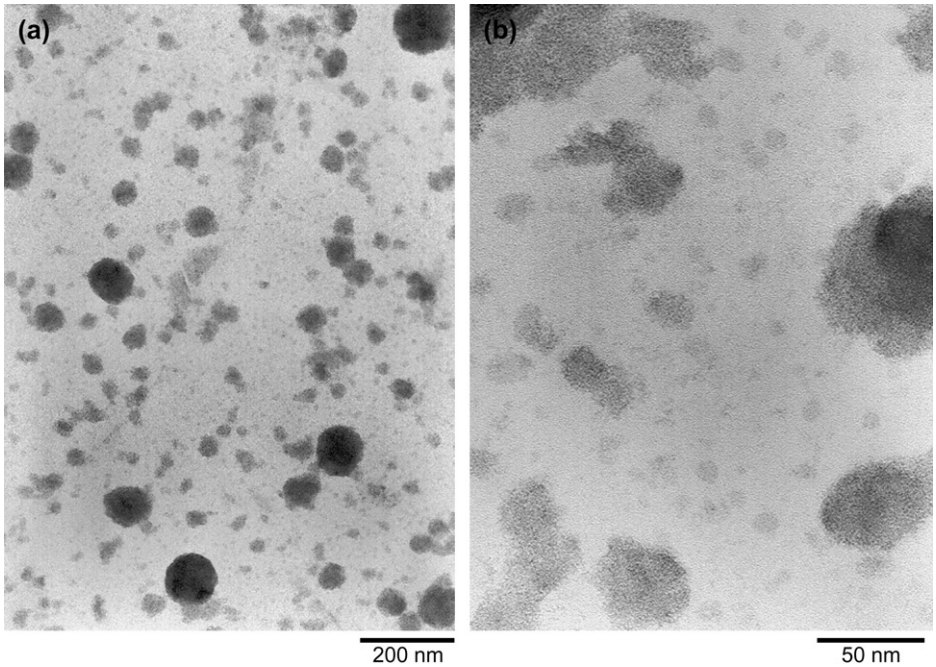

Fig. 2. TEM micrographs of *m*-PEEA with $x = 3$; the dark regions are the non-crystalline hard segments.

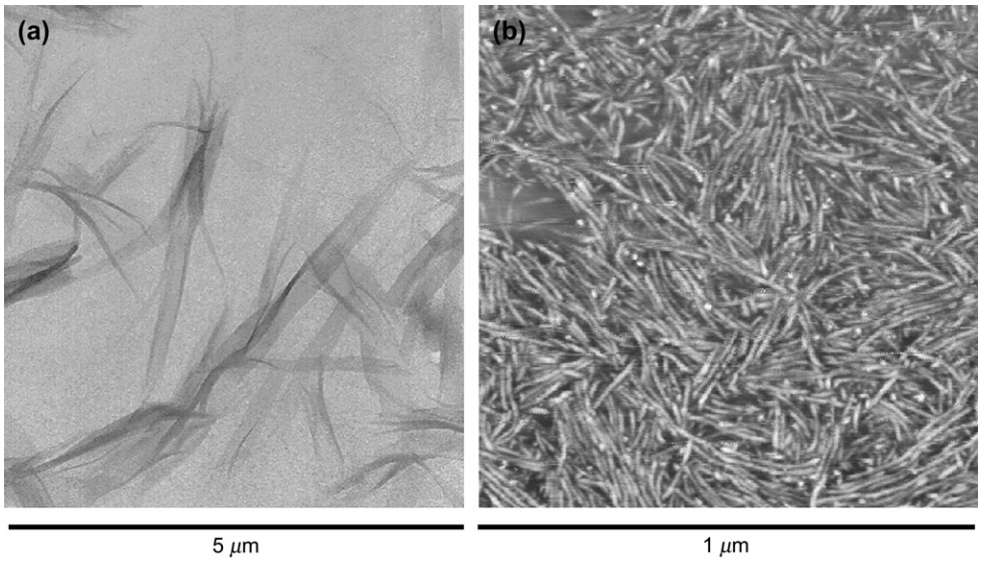

Fig. 3. (a) TEM and (b) AFM micrographs of 6-PEEA with $x = 2$; the grey ribbons are the hard segment crystallites.

3.1.2. p-PEEA and 6-PEEA

The segmented block copolymers with monodisperse crystallisable amide segments with a repeat length, x, of 1 and 2 displayed a transparent appearance in their melt state. At room temperature they were transparent solids. The melting temperature and heat of fusion of the amide segments were measured by DSC and the crystallinity was found to be high [13]. Thus, despite the short segment length and their low contents (12–26 wt%), the amide segments managed to crystallise rather well. The TEM micrographs revealed ribbon-like structures with thicknesses of a few nanometers and lengths of several micrometers (Fig. 3a). The crystallites thus displayed high aspect ratios ($\sim$1000).

For amide lengths of two repeat units, no spherical particles were observed and consequently no liquid–liquid demixed structures were present in these copolymers. The matrix was formed by the polyether segments containing some dissolved amide segments. A majority of the amide segments were phase separated into the crystallised, high-aspect-ratio ribbons.

A ribbon-like morphology was also observed by AFM (Fig. 3b). From the AFM micrograph, the thickness of the ribbons was estimated to be 5 nm and the length to be 200 nm. This was much shorter than what was seen with TEM. A probable explanation to this discrepancy was the fact that AFM only analyses the surface of a sample, whereas the ribbons were believed to extend below the surface and disappear from the viewing plane.

For 6-PEEA with a repeat length of 3, ribbon-like structures as well as small amounts of spherical particles were observed [13]. This suggests that liquid–liquid demixing had occurred. The major part of the phase-separated amide segments seemed to be present as crystalline ribbons. When viewing the samples with TEM and AFM, the AFM micrograph revealed narrower and more densely packed ribbons than that from TEM. However, the TEM analysis had been performed on very thin heat-treated films (50 nm), and the TEM results were thus expected to be less representative for the structure of the bulk.

In principle, segmented block copolymers have been obtained with liquid–liquid demixed morphologies (*m*-PEEA) (Fig. 4a) as well as with crystalline ribbons (*p*-PEEA and 6-PEEA) (Fig. 4b).

3.2. Dynamic mechanical analysis

The thermal mechanical properties of the segmented block copolymers were studied by DMA. As the PPO-based polyethers (*m*-PEEA) were amorphous, the glass transitions of the polyether phases were sharp and the flex temperatures were close to the glass transition temperatures (Fig. 5). The copolymers with crystalline ribbons (*p*-PEEA, 6-PEEA) displayed low values for T_g and T_{flex} and high values for T_{flow} as compared to the liquid–liquid demixed system (*m*-PEEA). In addition, the modulus between T_{flex} and T_{flow} was much less dependant on temperature. The storage modulus above T_g for the *m*-PEEA copolymers was strongly temperature dependant.

The glass transition temperatures of the PEEA copolymers were found to be independent of the amide content, as can be seen in Fig. 6.

The crystallised systems had similar T_gs which were low in temperature. The T_gs of the liquid–liquid demixed copolymers were approximately 10 °C higher than the crystallised systems. This suggests that a larger concentration of amide segment was dissolved in the polyether phase of *m*-PEEA. The amide segments in the *m*-PEEA had a random length distribution and were non-crystalline. The amide segments with a repeat length longer than 2 phase separated and the shorter segments dissolved in the ether phase. These dissolved short amide segments were expected to increase the T_g of the *m*-PEEA copolymers.

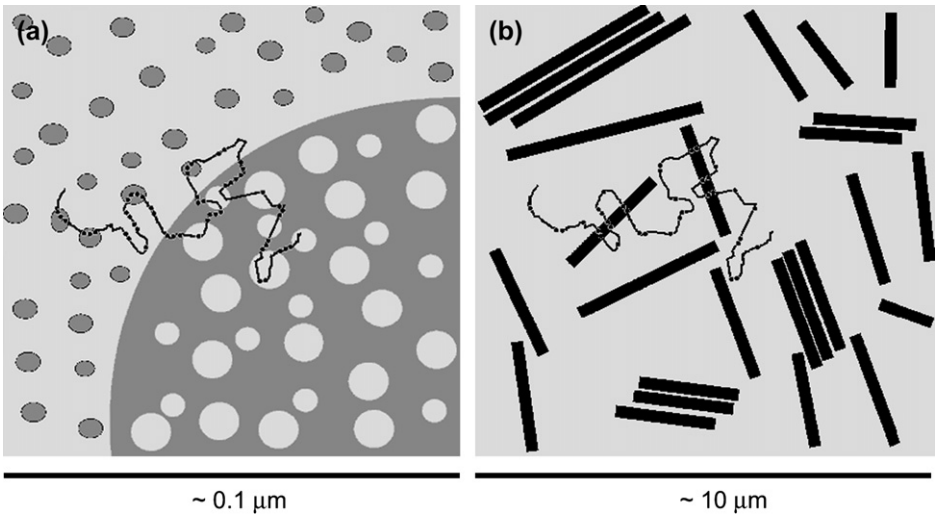

Fig. 4. Cartoons of PEEA morphologies displaying (a) liquid–liquid demixed particles and (b) crystalline ribbons. Note the large difference in scale.

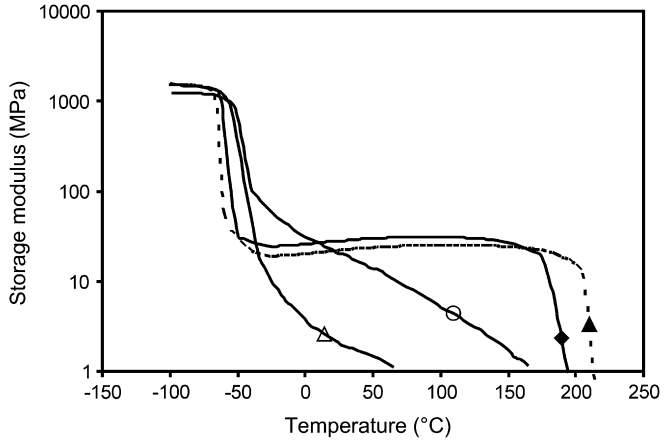

Fig. 5. The storage modulus as a function of temperature for *m*-PEEA $x = 3$, △; *m*-PEEA $x = 8$, ○; *p*-PEEA $x = 2$, ▲; 6-PEEA $x = 2$, ◆.

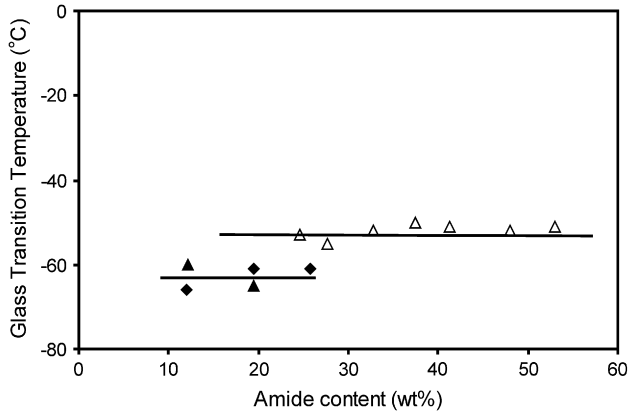

Fig. 6. The T_g of PEEA copolymers as a function of amide content for *m*-PEEA, △; *p*-PEEA, ▲; 6-PEEA, ◆.

The flex temperatures, defined as the onset of a low modulus, were approximately 15 °C higher than the T_g values for the crystallised systems, and 15–30 °C higher for the liquid–liquid demixed system (Table 1). Particularly the *m*-PEEA with shorter amide segments displayed high values of T_{flex}. The crystallised amide systems thus had appreciably enhanced low-temperature properties.

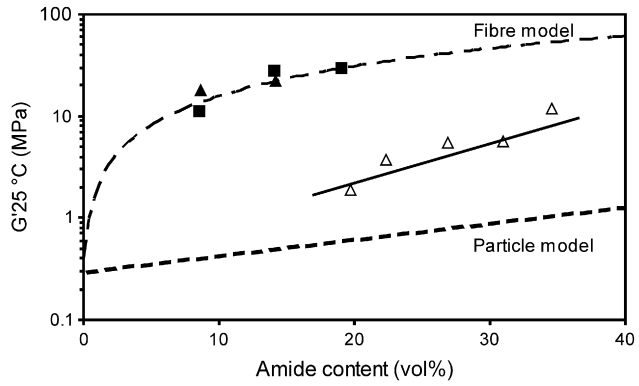

Fig. 7. Shear moduli at 25 °C as a function of amide content for *m*-PEEA, △; *p*-PEEA, ▲; 6-PEEA, ◆. The Guth–Smallwood relationship for particle-filled systems (particle model) [14] and the Halpin–Tsai relationship for fibre composites (fibre model) [13,15,16] are also presented.

The shear modulus at 25 °C for the systems with liquid–liquid demixed particles increased gradually with amide content (Table 1, Fig. 7).

For a system with filler particles the increase in modulus generally follows the Guth–Smallwood relationship (Eq. (3)) [14].

$$G^* = G^0\left(1 + 2.5\phi + 14.1\phi^2\right) \tag{3}$$

Here, G^* represents the composite modulus, G^0 the modulus of the base polymer (for PEO–PPO–PEO this value is 0.4 MPa) and ϕ the volume fraction of particles. The modulus of the *m*-PEEA copolymers displayed a more significant increase with amide content than was estimated by the Guth–Smallwood relationship. This might partly be due to the fact that the total volume of the particles was higher than the amide content as a result of the inclusion of PPO

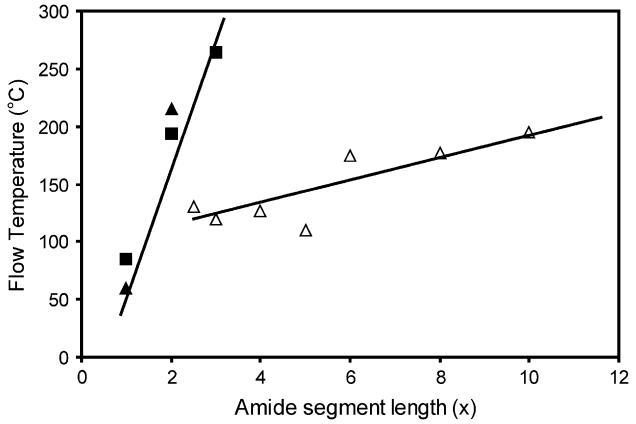

Fig. 8. The flow temperature of PEEA copolymers as a function of amide length for *m*-PEEA, △; *p*-PEEA, ▲; 6-PEEA, ◆.

segments in the submicron salami particles. However, this does not fully explain the discrepancy [11].

The moduli of the systems with crystalline ribbons were much higher than the particle-filled system. As the ester groups did not take part in the crystallisation, the amide content was calculated without the ester groups [20]. The *p*-PEEA and 6-PEEA had very similar storage moduli. These high moduli could be very accurately modelled with the Halpin–Tsai fibre composite model (Fig. 7) [13,15,16]. For this model, it was assumed that all the amide segments had crystallised, so that the modulus of the PEO–PPO–PEO phase was 0.4 MPa, the modulus of the crystalline phase was 5 GPa and that the aspect ratio of the crystallites was 1000. The *p*-PEEA and 6-PEEA displayed relatively high moduli despite their low amide contents. The reasons for this were the high crystallinity and the high aspect ratios of the crystallites [12,13]. Thus, crystallised structures seemed to be more efficient in increasing the modulus in the segmented block copolymers. It was remarkable that the moduli of copolymers with crystallised structures could be modelled with a fibre composite model, as this suggests that the moduli of the copolymers were functions of the structure of the phase-separated portion and that this portion thus could be regarded as a nanofiller phase.

The moduli of the liquid–liquid demixed system decreased gradually in the temperature range between T_{flex} and T_{flow} (Fig. 5). This decrease in modulus with temperature ($\Delta G'$) was of a much smaller magnitude for the crystallised systems with monodisperse segments (Table 1). The flow temperature for the liquid–liquid demixed system equalled the glass transition temperature, and for the crystallised systems it was the melting temperature of the amide phase. The value for T_{flow} was found to increase with amide segment length for both morphologies (Fig. 8).

The T_g of the amide phase in the liquid–liquid demixed system depended on the amide segment length and the amount of ether dissolved in the amide phase [11]. The T_m of the crystallised systems increased significantly with increasing amide segment length. It was expected that the amide segments were fully extended in the crystallites and that the crystal thickness should increase with amide segment length. Increasing the crystal thickness also increases the melting temperature [13,21,22]. Moreover, the content of the ether phase should have an effect [12,13] since it acts as a solvent for the crystallites and lowers the amide melting temperatures [17,18]. With these short amide segments the melting temperatures were already quite high.

3.3. Elastic properties

One of the most common tests for studying the elastic properties of a material is the compression set test (CS). The low strain properties are generally independent of molecular weight. The CS values of the PEEAs decreased strongly with increasing amide segment length, both for the liquid–liquid demixed system and the crystallised systems (Table 1, Fig. 9a).

The *p*-PEEA and 6-PEEA copolymers behaved in the same way. With increasing amide segment length, the thickness of

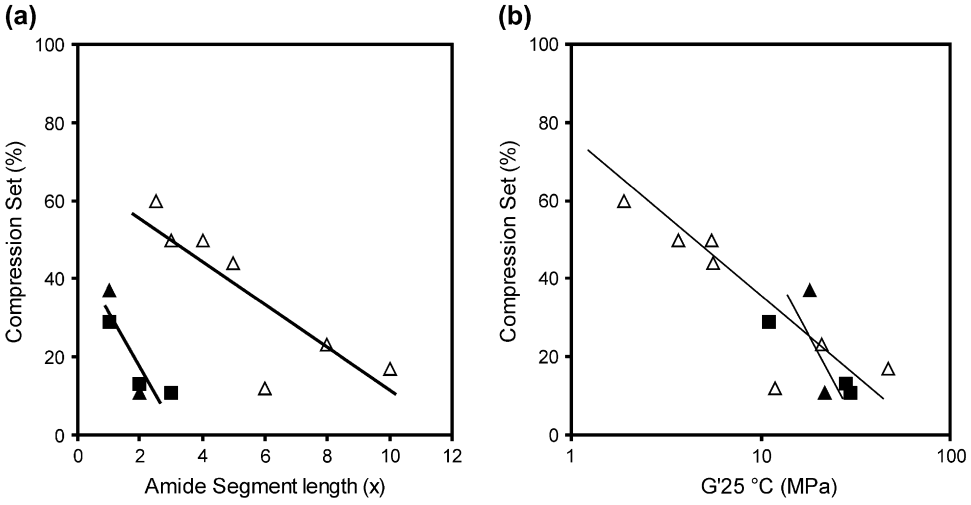

Fig. 9. The compression set of PEEAs as a function of (a) the amide segment length and (b) the storage modulus at 25 °C for *m*-PEEA, △; *p*-PEEA, ▲; 6-PEEA, ◆.

the phase-separated amide phase increased. This indicated that thick phases are more difficult to deform and that the copolymers with thicker crystallites or larger phase-separated domains have a more elastic behaviour. It was also remarkable that, for the same amide segment length, the CS values for the crystallised amide systems were much lower. Crystalline regions were apparently more difficult to deform than amorphous ones.

In the ASTM compression set test, the sample thickness was remeasured after remaining in an unstrained state for 30 min. This represented an arbitrary duration value. If the duration before remeasuring was increased, lower CS values would be obtained [12,13]. This decrease was more significant for the liquid–liquid demixed system than for the crystallised system. The liquid–liquid demixed systems were found to relax fully in 1–5 days [11], whereas the CS values for the crystallised system (*p*-PEEA) displayed a 50% reduction in one day [12]. This suggests that the elasticity of the liquid–liquid demixed system was better than the crystallised system after long time periods, whereas it was poorer after short time periods.

It is important for the materials to have a good elasticity at as high a modulus as possible. Generally the CS values of segmented block copolymers increase with increasing modulus [11]. However, for the studied copolymers, the opposite behaviour was observed (Fig. 9b). Longer amide segments were found to improve both the modulus and the compression set. It was interesting to observe that the CS values of the liquid–liquid demixed system and the crystallised systems did not differ that much in these conditions.

Another way of measuring a material's elasticity is with the tensile set test. In this test, a cyclic strain was applied, i.e. the strain was increased in steps and for each step the set was calculated [11–13]. A relevant one point value is the TS at 50% strain ($TS_{50\%}$) (Table 1). The $TS_{50\%}$ values for the studied copolymers were found to change in a similar manner to the CS values.

3.4. Direct comparison

Table 2 portrays a direct comparison of three PEEA copolymers with a storage modulus of about 20 MPa at room temperature (Table 2). These copolymers were the *m*-PEEA with eight amide repeat units and the *p*-PEEA and 6-PEEA with two monodisperse amide repeat units. In order to obtain a modulus value of 20 MPa, the hard segment content for the monodisperse crystallisable segments was about 20 wt% whereas approximately 50 wt% amide was required in the case of the liquid–liquid demixed system.

In the melt, the crystallised materials were homogeneous and at room temperature they maintained their transparent appearance. As a result of the homogeneous melts, the molecular weights of these copolymers were higher than if melt phasing had taken place. A high molecular weight of a material is important for its ultimate properties [17]. The low temperature properties T_g and T_{flex} were 10 °C lower for the crystallised systems as compared to the demixed one. This suggests that a lower amount of hard segments were mixed with the soft phase and thus that the phase separation by crystallisation was significant. Correspondingly, the crystallinity of the monodisperse crystallisable segments was high.

Table 2
Properties of segmented block copolymers with similar storage moduli at room temperature

	Crystal ribbons		Amorphous spheres
	6-PEEA	*p*-PEEA	*m*-PEEA
Amide repeat length (x)	2	2	8
Amide content (wt%)	19.4	19.5	48
Inherent viscosity (dl/g)	1.03	1.14	0.87
Appearance	Transparent	Transparent	Non-transparent
Storage modulus (MPa)	28	22	21
Loss modulus (MPa)	0.3	0.1	3
Tan δ	0.011	0.0045	0.14
$\Delta G'$ (10^{-3}/°C)	0	0	11
T_g (°C)	−61	−64	−52
T_{flex} (°C)	−46	−53	−35
T_{flow} (°C)	194	215	180
$CS_{25\%}$ (%)	13	11	23
$TS_{50\%}$ (%)	17	19	21

The flow temperatures of the three materials were similar. The temperature dependence of the modulus ($\Delta G'$) was much lower for the crystallised copolymers as was the temperature dependence of the loss modulus and the loss factor. A constant modulus over a large temperature range combined with a low T_g was observed, indicating an excellent low temperature behaviour. The low values for the loss modulus (G'') and loss factor (tan δ) suggested that the dynamic properties were appreciably enhanced. Surprisingly, the elastic properties (CS and TS) did not differ that much between the three materials and were only marginally enhanced with the monodisperse hard segments.

The melt rheological behaviour and the rate of solidification on cooling were not part of the present investigation but are important parameters to study. A homogeneous melt phase usually has a lower melt viscosity and a less elastic melt than a melt with liquid–liquid demixed particles. The solidification on passing the T_g and on crystallising with monodisperse segments are both fast processes. For systems with similar moduli, the advantages of monodisperse crystallisable segments over the liquid–liquid demixed segments were not very apparent with respect to the elastic properties (CS). However, regarding the low temperature, the dynamic behaviour and the attainability of high molecular weights, they were found to be superior. The fact that they were transparent was also an advantage.

4. Conclusions

The properties of segmented block copolymers with either liquid–liquid demixed or crystallised structures were compared. The liquid–liquid demixed system displayed a morphology consisting of nanoparticles containing only rigid segments in addition to submicron particles with salami type, phase-inverted structures. The crystallised structure was built up of

crystallisable segments with monodisperse segment length distributions and the morphology consisted in nanoribbons with high aspect ratios (1000).

The copolymers with the nanocrystallised structures were transparent and had higher molecular weights than the liquid–liquid demixed systems. The crystallised segments were more efficient in increasing the modulus as well as in increasing the elasticity (decreasing the CS and TS). Moreover, the glass transition temperature of the polyether phase in the crystallised systems was lower, suggesting a lower dissolution of rigid segments. This resulted in better low temperature properties. The storage modulus (G') was temperature independent and, in relation to this, the loss modulus (G'') and the loss factor (tan δ) were very low. Even the storage modulus seemed to increase with temperature as for an ideal rubber, the low loss factor suggested very good dynamic properties for the materials with crystallisable segments. The hard phase in segmented block copolymers should thus preferably be crystalline.

The increase in modulus for the systems with crystallisable segments could be accurately described with a model based on fibre reinforcement and at low strains the system could be regarded as reinforced with high aspect ratio nano-fibres. The rigid segments in the liquid–liquid demixed system had complex particle morphologies and the increase in modulus was somewhat better than what could be expected of a particle-filled system.

Acknowledgments

This research was financed by the Dutch Polymer Institute (DPI, The Netherlands) project #137. The authors would like to thank Professor Dr. J. Feijen, Dr. E. van der Heide from Shell, Amsterdam, and Dr. H.J.M. Gruenbauer from DOW, Terneuzen, for fruitful discussions.

References

[1] Holden G, Legge NR, Schroeder HE. Thermoplastic elastomers: a comprehensive review. 1st ed. Munich: Hanser Publishers; 1987.
[2] Fakirov S. Handbook of condensation thermoplastic elastomers. Weinheim: Wiley-VCH; 2005.
[3] Bayer O. Mod Plast 1947;24:250–62.
[4] Frisch KC, Saunders JH. Polyurethanes: chemistry and technology: part I chemistry. In: Mark H, Flory PJ, et al., editors. High polymers, vol. 16. New York: John Wiley & Sons; 1964.
[5] Armistead JP, Wilkes GL. J Appl Polym Sci 1988;35:601–29.
[6] Leibler L. Macromolecules 1980;13:1602–17.
[7] Li Y, Desper R, Chu B. Macromolecules 1992;25:7365–73.
[8] Koberstein JT, Russel TP. Macromolecules 1986;19:714–20.
[9] Elwell MJ, Ryan AJ, Gruenbauer HJM, Van Lieshout HC, Lidy W. Plast Rubber Compos Process Appl 1995;23:4.
[10] Frisch KC, Saunders JH. Polyurethanes: chemistry and technology: part II technology. In: Mark H, Flory PJ, et al., editors. High polymers, vol. 16. New York: John Wiley & Sons; 1964.
[11] van der Schuur MJ, van der Heide E, Feijen J, Gaymans RJ. Polymer 2005;46:3616–27.
[12] van der Schuur MJ, de Boer J, Gaymans RJ. Polymer 2005;46:9243–56.
[13] van der Schuur MJ, Gaymans RJ. J Polym Sci Part A 2006;44:4769–81.
[14] Guth E. J Appl Phys 1945;16:20–5.
[15] Halpin JC, Kardos JL. J Appl Phys 1972;43:2235–41.
[16] Guan X, Pitchumani R. Polym Eng Sci 2004;44:433.
[17] Niesten MCEJ, Feijen J, Gaymans RJ. Polymer 2000;41:8487–500.
[18] Krijgsman J, Husken D, Gaymans RJ. Polymer 2003;44:7573–88.
[19] van der Schuur MJ, Feijen J, Gaymans RJ. Polymer 2005;46:327–34.
[20] Niesten MCEJ, Harkema S, van der Heide E, Gaymans RJ. Polymer 2001;42:1131–42.
[21] Sperling LH. Introduction to physical polymer science. 3rd ed. New York: John Wiley and Sons; 2001.
[22] Niesten MCEJ, Gaymans RJ. Polymer 2001;42:6199–207.